Multi-Axis FDM 3D Printing

Yonatan Morocz, Doctoral Student at the Juncker Lab

1 Introduction

Additive Manufacturing (AM) has evolved from a niche specialized technology to a mainstream tool used by engineers and scientists but also artists and creatives in many possible fields. The reasons behind this are AMs unique ability to conserve both material and time compared to other fabrication methods as well us unlocking geometries and workflows previously unattainable. While traditional subtractive and forming technologies may benefit from the economies of scale, AM has the versatility to perform for small to medium batch production. Further innovations in the field of AM will come not just from technical and materials discoveries but also in the field of process optimization and toolpath algorithms.

The range of AM technologies has evolved drastically since their inception in the 1980s, now incorporating powder, liquid and solid substrates for fabrication. Most of these approaches involve the segmentation of a model into slices perpendicular to a primary build vector. This primary building direction will dictate the mechanical properties and tolerances of the printed component.[2, 15] Fused Deposition Modelling (FDM) is the most common embodiment of AM currently, which relies on the extrusion of thermoplastics such as acrylonitrile butadiene styrene (ABS) or polylactides (PLA). This paper focuses on expanding the abilities of FDM past the limitations of traditional 3-axis printing without incurring the complexity and challenges of a true multi-axis configuration.

1.1 Limitations of Traditional 3-Axis FDM:

Current state-of-the-art FDM printers limit themselves to one principal build direction within a three axis movement system. The construct is subdivided into layers of uniform thickness, perpendicular to the principal build vector. These layers can then be fabricated sequentially in a repetitive 2D printing approach to create a final 3D construct. This approach lends itself to facile algorithmic slicing and general automated model to G-code pipelines. Standard 3-axis slicing and printing was adopted primarily due to its simplicity and sufficiency for many AM tasks. However, this approach results in anisotropic material properties, the stair-step effect on part surfaces and limits the user to specific printable geometries or the use of supports.

FDM is inherently an inhomogeneous method as it extrudes material in planes, creating interfaces between newly extruded material and the previous layer. This causes the aforementioned anisotropic behaviors observed in traditional FDM prints, with lower material strength at these interfaces than within the direction of filament extrusion. There exist approaches to mediate this print-orientation dependent effect such as differential z offset of neighboring deposition traces.[10] Such methods can reduce the anisotropic nature of a part, but don't provide full control over the strength in different axes.

Another fundamental effect of FDM printing is the difference between the XY resolution and the Z resolution, stemming from the separation of the construct into discrete Z layers. In the XY plane an FDM printers resolution is limited by its nozzle size and motion system accuracy while in the Z axis the size of the slices is the limited factor. More important is that in XY the instrument can interpolate between two positions while in Z it cannot, the extrusion is constrained within either the previous or the current slice during printing. This results in a discrepancy between the surface finish depending on which axes the surface slopes against. Shallow sloped surfaces along the Z axis suffer from this "stair-step" effect most prominently.

A physics-based limitation of 3-Axis FDM printing is the inability to print in mid air, or extrude molten material in a position without adequate support. In this case the molten material is not constrained to the intended geometry and can result in incorrect part tolerances and inferior mechanical properties. This behavior can be further subdivided into; overhangs, bridging and mid-air printing. Achievable overhang angles can be improved through clever toolpath implementations or more powerful cooling to prevent material droop. Similarly bridging can be ameliorated through proper toolpath control and precise tuning of extrusion temperature and cooling rates. Mid-air printing however has no facile fix apart from changing the principal printing vector so that the desired structures are no longer printing in mid-air. The effect of different printing methods on these geometries is highlighted in Fig.1:**D**)

Additional printed constructs called supports provide a base for overhangs above a printable angle and mid air prints. These sacrificial materials increase the print time and material consumption while reducing the surface quality at their interface. There are alternative support materials such as water soluble PVA for easier cleanup, however this raises an entirely other host of challenges associated with successful and rapid multi-material printing.

The limitations described herein result from the fundamentals of the 3-axis FDM process. Multi-axis FDM effectively counters each of these.

1.2 Challenges of Multi-Axis FDM

Multi-Axis FDM utilizes multiple or variable principal build directions to circumvent the challenges facing 3-Axis printers. There are a great variety of multi-axis embodiments, each with their own set of advantages and specific abilities.[12, 11, 5, 1] A common design involves the addition of a fourth and fifth axis either through a rotating Z substrate or a rotating and tilting print head. However, there are plenty of more complex embodiments which can add further axes to such instruments.

Adding further axes lead to more complex machinery and control software. Completely custom configurations are often built because the alternatives are exorbitantly expensive. However, these custom configurations often lack the adaptability and ease of use to become mainstream. The knowledge and practice required to build such a system from the ground up poses a significant barrier to entry for non-experts in the field.

The slicing of a 3D object into printer Gcode is another limiting frontier currently facing the widespread adoption of multi-axis 3D printing. While there have been many algorithmic approaches which successfully simplified the slicing process, these are often tailor made for the specific machines they are used on.[13, 9, 4, 16, 7] Allowing tool-path planning to consider extra dimensions exponentially increases the possible approaches to a fabrication step.[18] There are no slicing algorithms yet for multi axis printing capable of choosing the correct approach to achieve

the desired mechanical or tolerance result for general geometries. The specific limitations of a printer are also a huge factor which if not considered can cause instrument damage and production delays. Trajectory planning becomes more complex as you consider variables such as collision with structural and printed components.[14]

The Multi-Axis slicing and printing workflow presented here allows the user to capitalize on the benefits of multi-axis printing without incurring the costs or complexity of other solutions.(Fig.1:**A**) By leveraging standard 3-Axis printer hardware and widespread 3-Axis slicing software and settings this approach can be executed by any 3D printer to recreate pseudo multi-axis geometries.[17] The basic principle of this approach is to use the internal coordinate system of the printer to fabricate locating and work-holding components which will then interact with the final construct as it is being printed. In the example presented in Fig.1:**E**, the original substrate is printed first (black), then removed from the build plate. The the work-holding component (white) is printed and the original substrate is placed into it. This means that the printer now knows where the original substrate is despite the fact that it was printed and then removed from the bed. Now the printer is able to return and deposit new material along a principle axis that differs from that of the original substrate. In this manner a construct can be assembled with many principle build axes and their associated mechanical properties. A comparison between different embodiments of FDM printing are shown in Fig.1:**C**, highlighting the characteristics where the multi-axis approach outperforms the others.

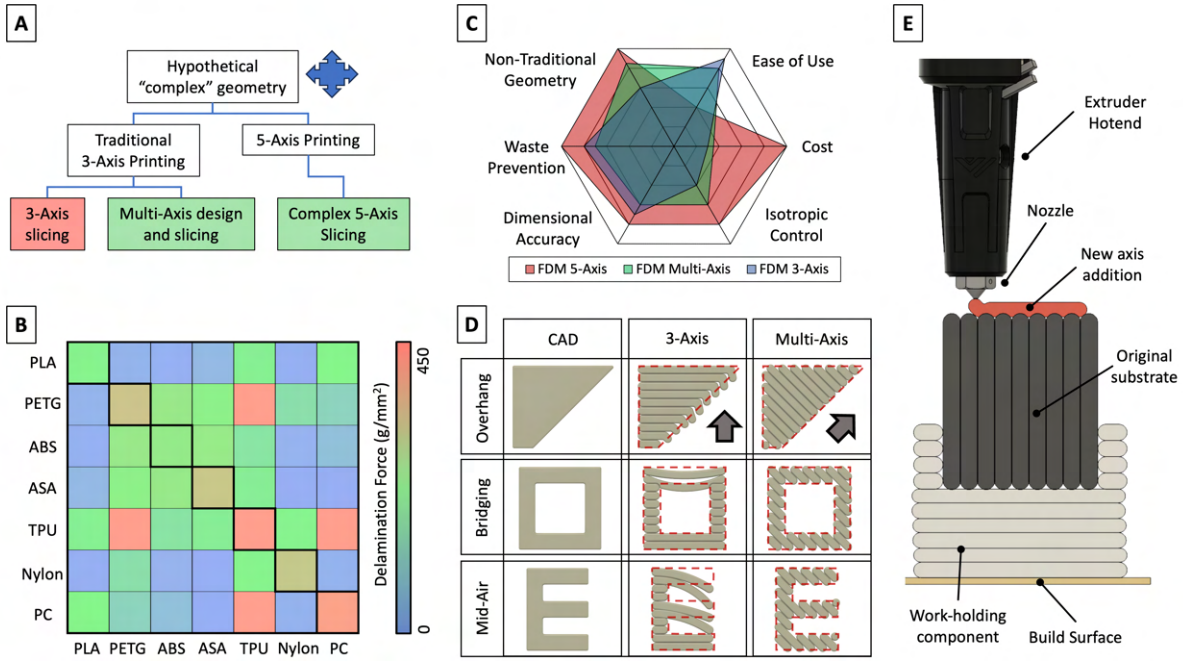

Figure 1: **A)** Fabrication options for a hypothetical complex geometry. (Red=cannot be fabricated, Green=can be fabricated) **B)** Interfacial stability and printability of common thermoplastic materials. **C)** Comparison between 3-Axis FDM, 5-Axis FDM, and Multi-Axis FDM. **D)** Illustrating the effect of print orientation on final part tolerance and printability. **E)** An illustration of the in-situ work-holding and printing.

2 Results

2.1 Multi-Axis cube

To prove the initial concept a multi sided cube was designed which cannot be printed without support material and/or compromised structural integrity. Pre-planned printing steps and print-in-place work-holding allow this part to be fabricated without any supports with reproducible tolerances and stronger interfaces. The work-holding component was designed to hold both the single cube and the cube configuration in fig.2:5-6.

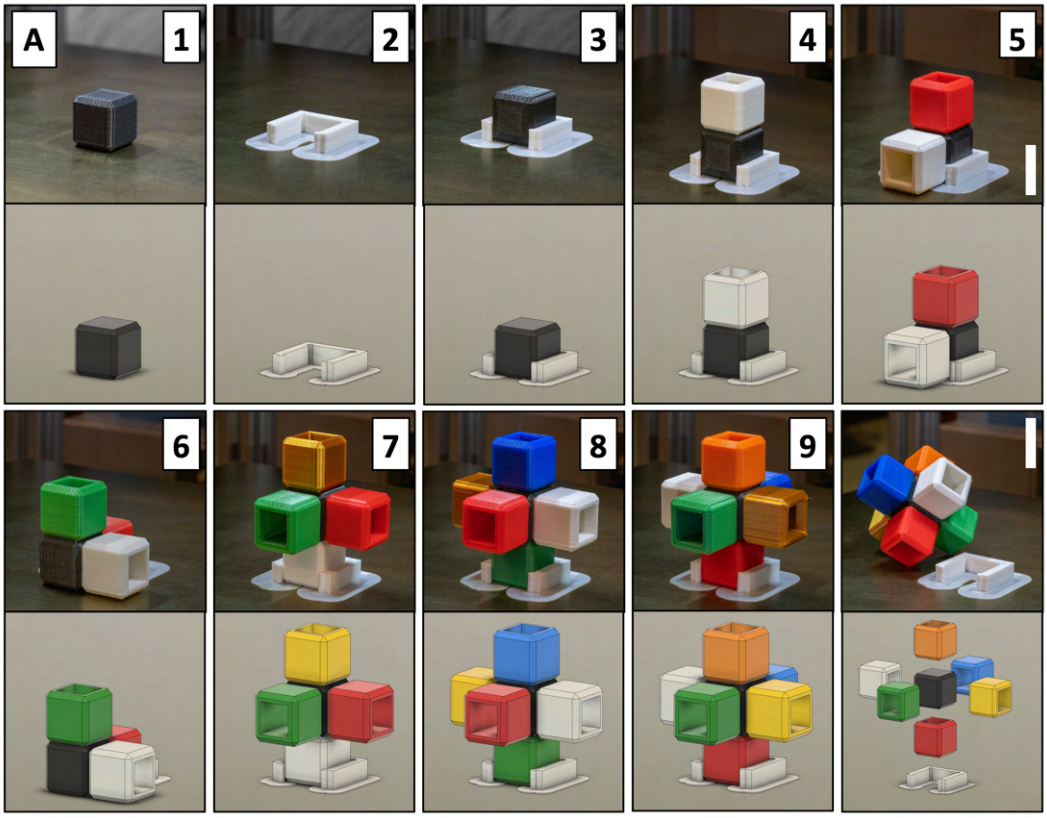

Figure 2: Fabrication steps of the multi-axis cube. (Above) photos of print. (Below) CAD rendering. (scale bar = 20 mm)

Overall the dimensions were within 100-200 μm for single cubes as expected, but the three cube external and diagonal cube assembly had worse dimensional errors. (Fig.3) During steps 7-9 in the fabrication process the printing is occurring farther above the mounting point, This causes a slight flex of the part, allowing the dimensions to vary slightly from the designed tolerances.

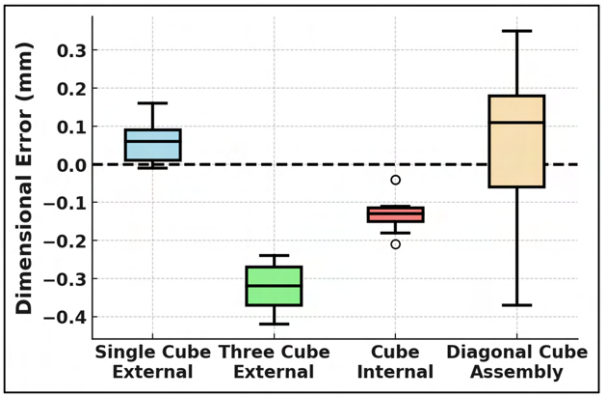

Figure 3: The dimensional error for different aspects of the multi-axis cube.

2.2 Facile work-holding configurations

To fix the previous issues regarding part holding, multiple facile work holding structures were tested to determine the most reliable attachment method for further operations. The 5 configurations tested were: **A)** Friction based attachment similar to that used in the previous demonstration. This technique showed large variability, with a dimensional error centered around 240μm. **B)** Bolted attachment through pre-designed alignment holes. This method had the lowest variability of any method (90 μm) making it an ideal candidate for larger projects. **C)** Dovetail attachment inspired by woodworking jointry, this method allows for rapid and rigid mounting with a **D)** Angled substrate mount (friction). **E)** Angled substrate mount (friction). The last two conditions were variants of the initial friction work-holding redesigned for diagonal and conformal mounting of parts.

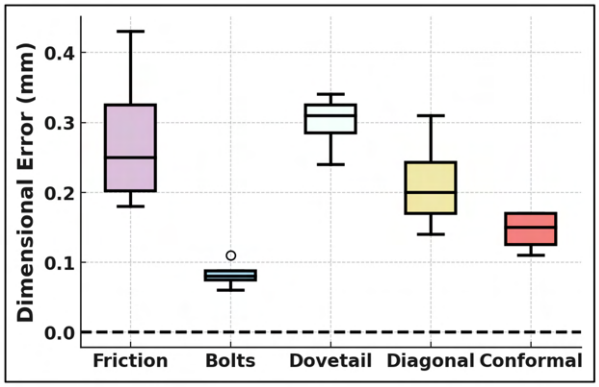

Figure 4: The dimensional error of varied work-holding configurations.

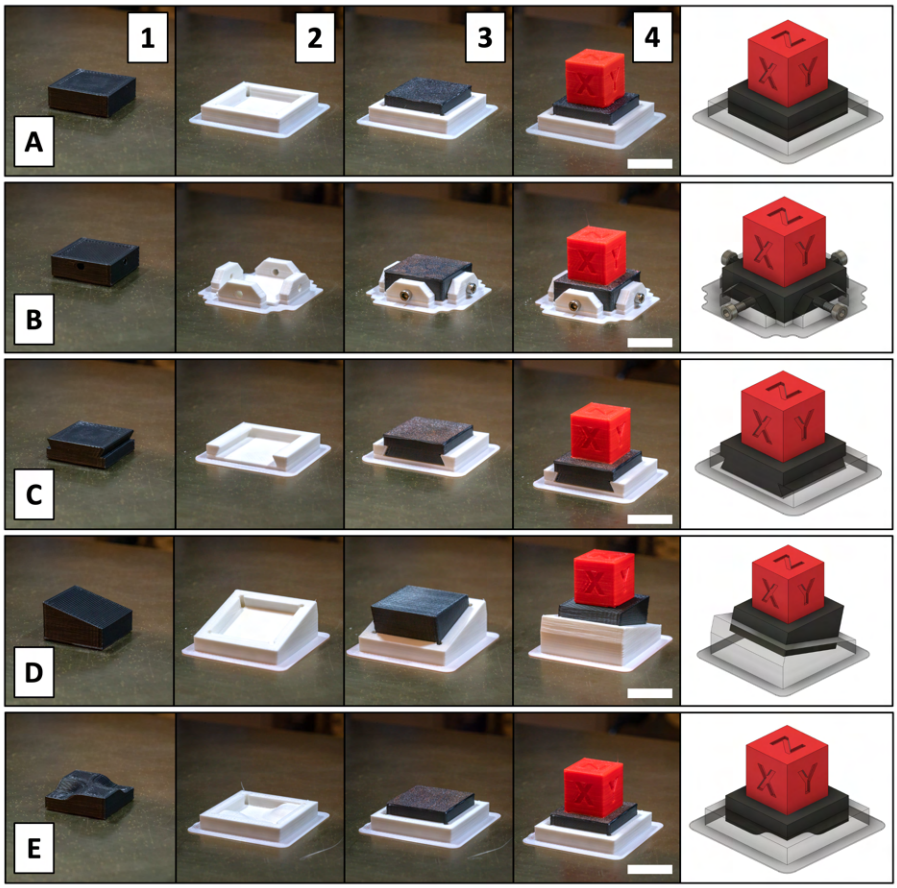

Figure 5: Several work holding configurations for flexibility in part attachment. The black substrate is printed first followed by the white mount, then the substrate is attached to the mount through various methods, finally the red cube is printed onto the substrate. **A)** Friction based attachment. **B)** Bolted attachment. **C)** Dovetail attachment. **D)** Angled substrate mounting (Friction). **E)** Conformal substrate mounting (Friction).

Drawing inspirations from other fields could lead to many improved work-holding configurations for better tolerances or part manipulation. The designs presented herein were chosen due to their adaptability to a large number of part geometries and constraints as well as their relative simplicity and low material cost. The next demonstration highlights a configuration where a more complex and costly work-holding construct is required.

2.3 Turbine Blade Demonstration

The multi axis work-holding was taken a step further through innovative part mounting with heat inserts for precise rotation. The parts were printed in the order shown in Fig.6. The blade thickness was within 50 μm of the designed part while the blade radius and the blade length had larger errors or 300 μm. More complex parts require planning in the design phase to optimize components for facile multi-axis printing. During this fabrication process due to a miscalculation during the path planning there was a collision between the nozzle and the work-holding. This resulted in a detachment of the work-holding piece in white from the build platform. However, since the

coordinate system is conserved, the work-holding component was reprinted and the substrate re-mounted. The printing was then resumed from the previous step without loss of tolerance or part progress. Since the localization of the part is dependent on the work-holding component, any misalignment can be corrected easily.

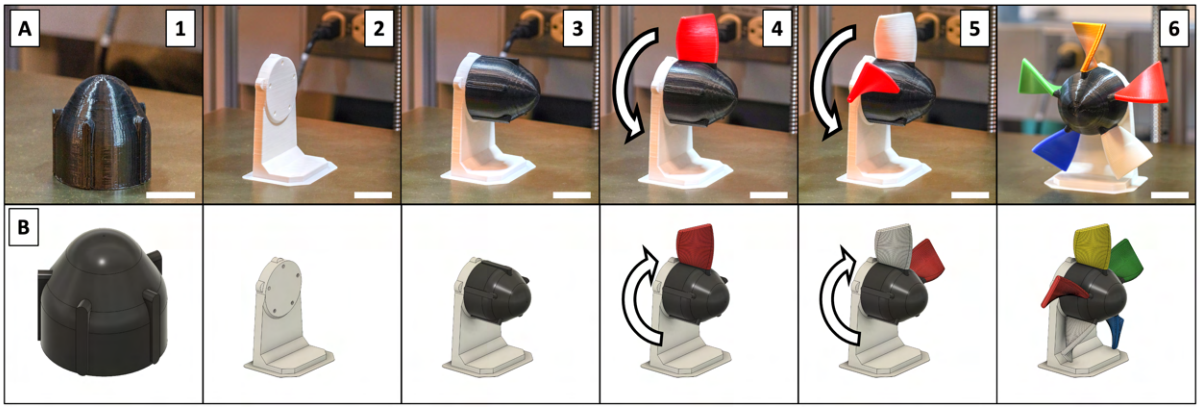

Figure 6: Fabrication of a turbine blade. **A)** The assembly steps for the turbine. 1) Print the core of turbine. 2) Print work-holding component. 3) Turbine core attached to the work-holding component. 4) First blade printed onto the turbine core. 5) Rotated by 72 degrees and printed second blade. 6) Final 5 fin design for turbine. (Above) photos of print. (Below) CAD rendering. **B)** Computer renderings of the procedure described in A.

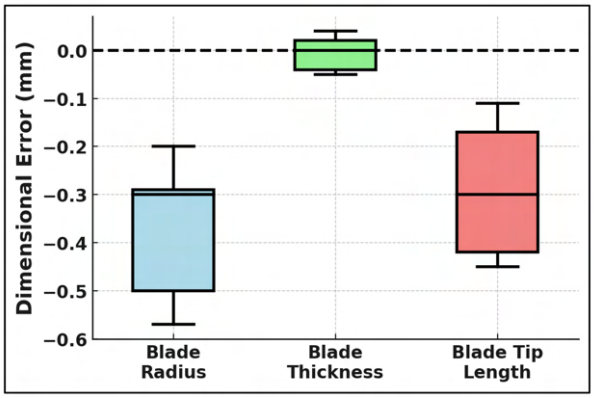

Figure 7: The dimensional error for different aspects of the turbine blade demonstration.

Further embodiments with multi-location mounting for more complex structures can provide more precise and rigid positioning. This technique of breaking the part down into principal axes and printing through work-holding positioning allows access to advanced geometries and closer control over the material anisotropy. The basic principle demonstrated herein can be taken much further to assemble large multi-material constructs.

To evaluate potential multi-material candidates we conducted straightforward testing of the adhesion strength between commonly used FDM material combinations. Several material combinations stood out with poor performance, while a few had extremely strong interfacial bonding.

PLA did adhesion was average for TPU and PC, but very weak for PETG, ABS and ASA. Nylon worked well with TPU and even better with itself, but poorly with most other materials. PC had extremely strong adhesion with TPU and itself, but relatively poor adhesion with many of the other materials. Specifically 4 material combinations stood out with delamination forces above $300\ g/mm^3$ (TPU:TPU, PC:PC, TPU:PC, and TPU:PETG).

3 Methods

3.1 Multi-Material Interfaces

Multi material samples were printed vertically to simulate the weakest possible adhesion scenario, predisposing the samples to delamination. The comparison matrix of which materials worked well with each other is shown in Figure. 1, and the individual data points are shown in Figure. 9.

The following test samples were printed on a Voron 0.1 FDM 3D printer in a fully enclosed chamber to maintain ambient temperature. The hotend utilized was a Dragon High Flow (Phaetus), paired with the mini afterburner extruder and toolhead. Prints were executed at 50 mm/s print speeds with 5,000 mm^2/s acceleration. The hotend was primed with 50 mm of extrusion prior to printing at the multi-material interface to ensure full contact throughout the interface. [8, 3, 6, 19, 20, **?**]

Material	Nozzle Temp	Bed Temp	Fan Power
Polylactic Acid (PLA)	220 C°	60 C°	80%
Polyethylene terephthalate glycol (PETG)	250 C°	80 C°	30%
Acrylonitrile Butadiene Styrene (ABS)	250 C°	100 C°	20%
Acrylonitrile styrene acrylate (ASA)	250 C°	100 C°	20%
Thermoplastic polyurethane (TPU)	240 C°	60 C°	20%
PA6 GF Nylon	275 C°	100 C°	20%
Polycarbonate (PC)	290 C°	100 C°	20%

The testing was conducted with the device shown in figure.9, wherein the sample was attached to two hooks and underwent increasing tension until delamination occurred.

3.2 Multi-Axis Printing

Multi-Axis printing demonstrations were exported as STL files (Fusion360) with labelled objects where the different parts could be sliced separately (Cura). Then the components were printed and oriented according to the pre-planned fabrication steps. The printer utilized was a custom built HevORT printer with a Goliath (VZBot) long melt zone hot-end (Fig.8). The parts were printed from PLA at the temperatures and speeds indicated in section 3.1. The parts were measured with calipers at the locations indicated in the measuring diagrams in Fig.10-12.

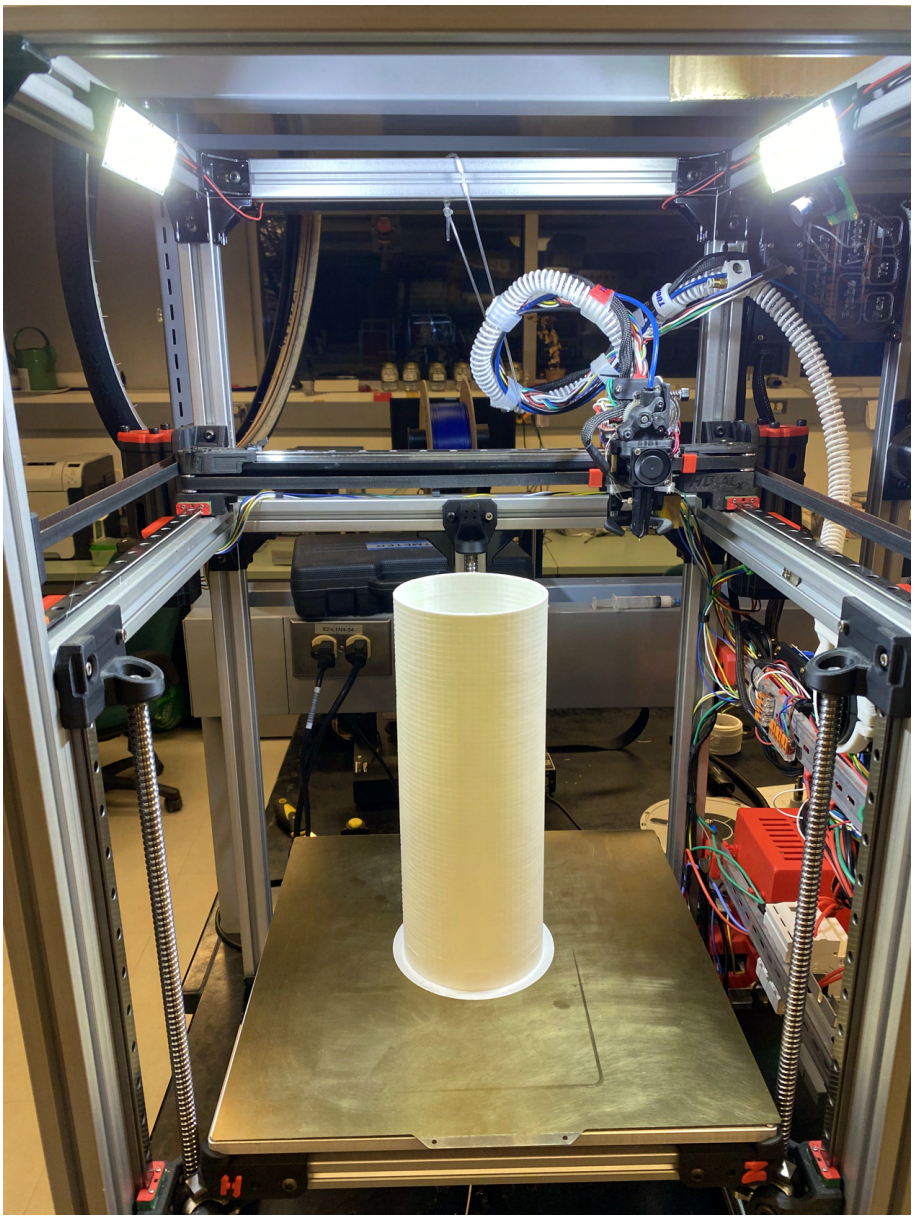

Figure 8: HevORT printer utilized in the multi-axis demonstration prints.

4 Supplementary

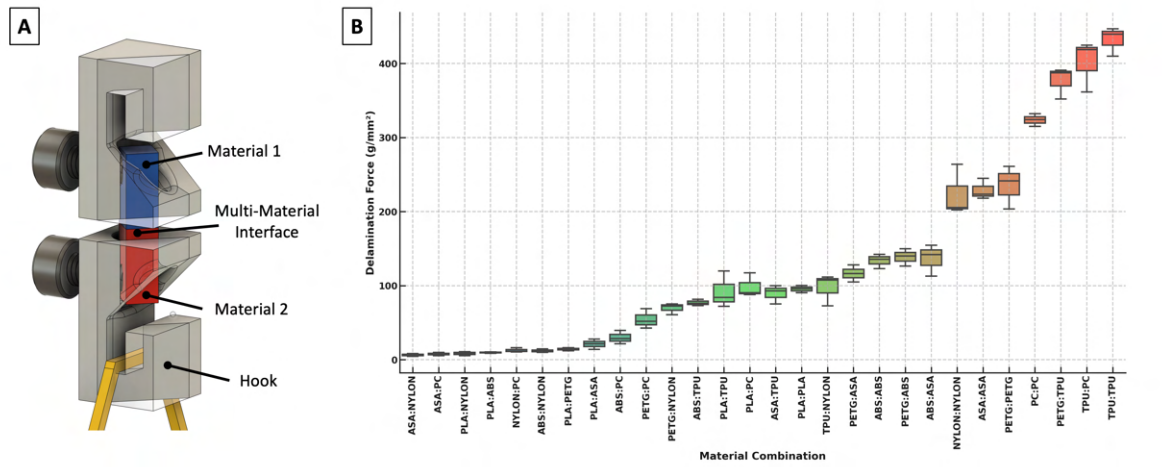

Figure 9: **A)** The measurement configuration for multi-material interface testing. Samples were mounted into the grippers and then pulled apart by increasing force until mechanical failure. **B)** A plot of the delamination forces for different material combinations. (N=3)

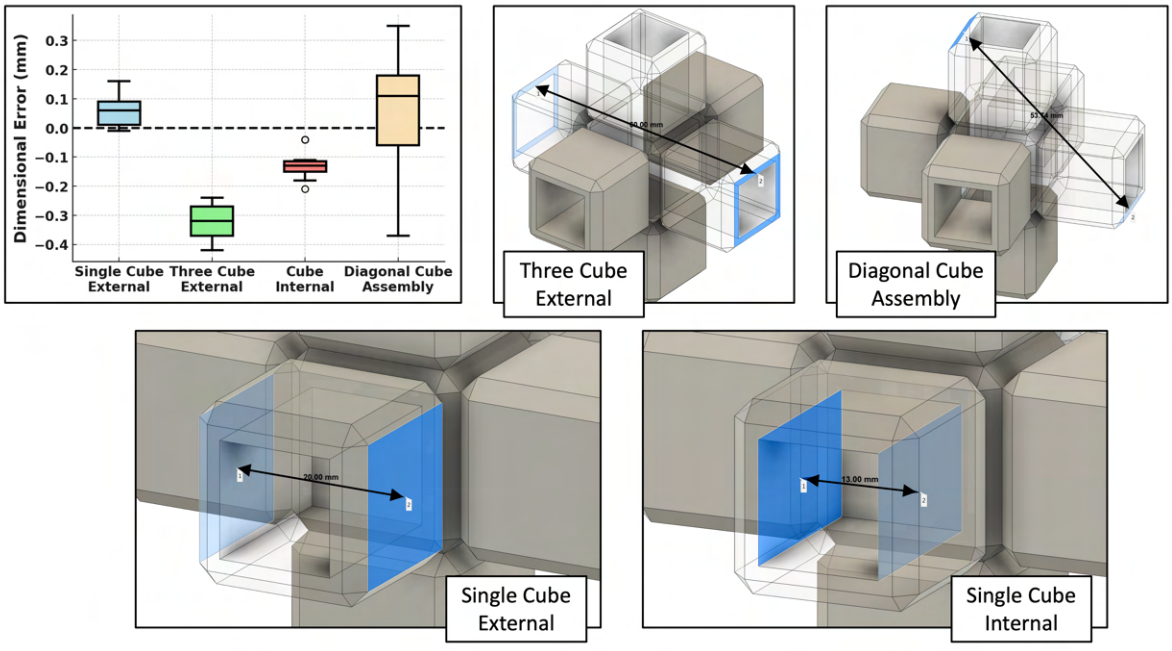

Figure 10: Measurement positions and results from multi cube demonstration.

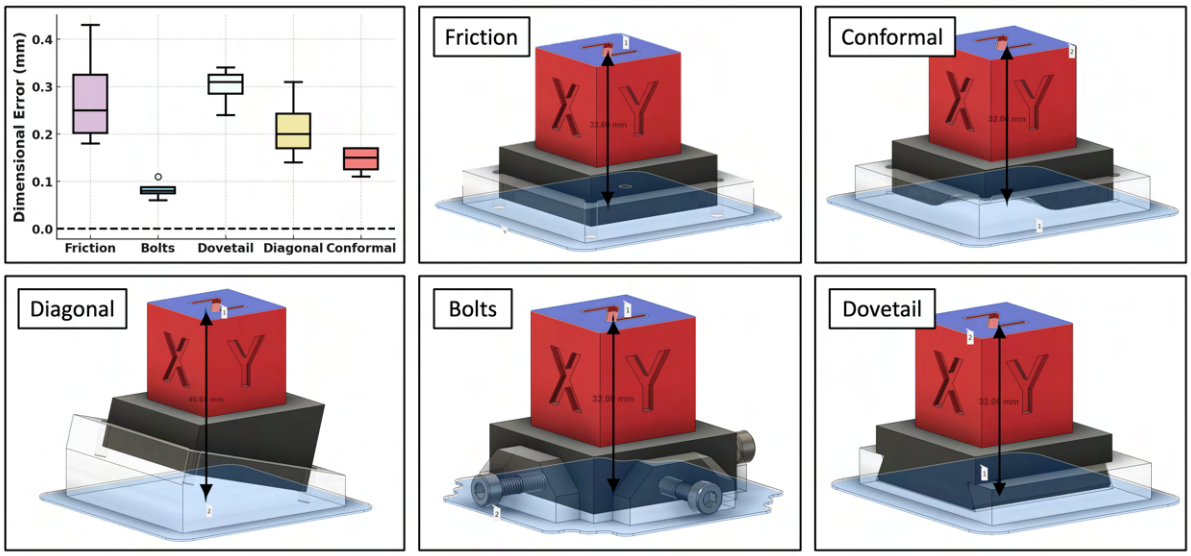

Figure 11: Measurement positions and accuracy of different workholding configurations.

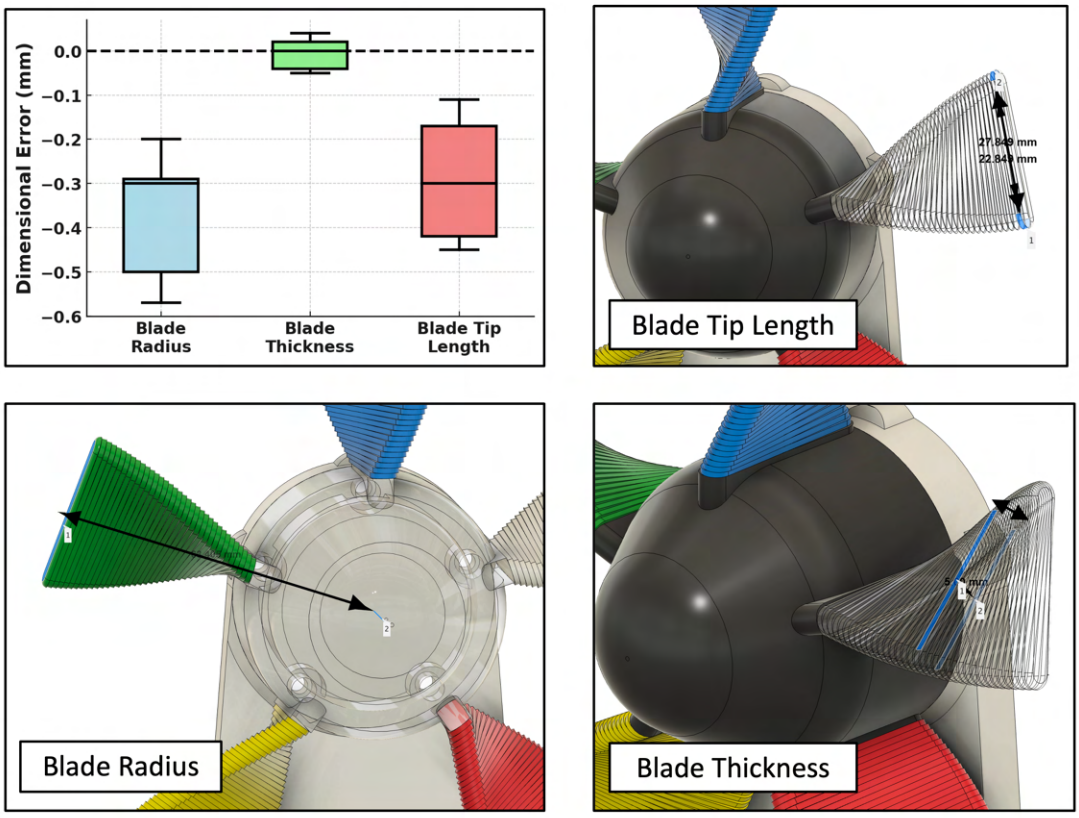

Figure 12: Measurement positions and accuracy of the turbine blade demonstration.

References

[1] J. J. Adams, E. B. Duoss, T. F. Malkowski, M. J. Motala, B. Y. Ahn, R. G. Nuzzo, J. T. Bernhard, and J. A. Lewis. Conformal printing of electrically small antennas on three-dimensional surfaces. *Advanced Materials*, 23(11), 2011.

[2] S.-H. Ahn, M. Montero, D. Odell, S. Roundy, and P. K. Wright. Anisotropic material properties of fused deposition modeling abs. *Rapid prototyping journal*, 8(4):248–257, 2002.

[3] M. Andó, M. Birosz, and S. Jeganmohan. Surface bonding of additive manufactured parts from multi-colored pla materials. *Measurement*, 169:108583, 2021.

[4] P. M. Bhatt, R. K. Malhan, P. Rajendran, and S. K. Gupta. Building free-form thin shell parts using supportless extrusion-based additive manufacturing. *Additive Manufacturing*, 32:101003, 2020.

[5] P. M. Bhatt, R. K. Malhan, A. V. Shembekar, Y. J. Yoon, and S. K. Gupta. Expanding capabilities of additive manufacturing through use of robotics technologies: A survey. *Additive manufacturing*, 31:100933, 2020.

[6] E. Brancewicz-Steinmetz, R. Valverde Vergara, V. Buzalski, and J. Sawicki. Study of the adhesion between tpu and pla in multi-material 3d printing. *Journal of Achievements in Materials and Manufacturing Engineering*, 115(2), 2022.

[7] D. Chakraborty, B. A. Reddy, and A. R. Choudhury. Extruder path generation for curved layer fused deposition modeling. *Computer-Aided Design*, 40(2):235–243, 2008.

[8] R. N. M. Delda, B. J. Tuazon, and J. R. C. Dizon. Assessment of interfacial adhesion of adhesively bonded 3d-printed thermoplastics. In *Materials Science Forum*, volume 1005, pages 157–165. Trans Tech Publ, 2020.

[9] G. Fang, T. Zhang, S. Zhong, X. Chen, Z. Zhong, and C. C. Wang. Reinforced fdm: Multi-axis filament alignment with controlled anisotropic strength. *ACM Transactions on Graphics (TOG)*, 39(6):1–15, 2020.

[10] S. Hermann. Brick layers. making prints stronger., Feb 2024.

[11] F. Hong, S. Hodges, C. Myant, and D. E. Boyle. Open5x: Accessible 5-axis 3d printing and conformal slicing. In *CHI Conference on Human Factors in Computing Systems Extended Abstracts*, pages 1–6, 2022.

[12] F. Hong, B. Lampret, C. Myant, S. Hodges, and D. Boyle. 5-axis multi-material 3d printing of curved electrical traces. *Additive Manufacturing*, 70:103546, 2023.

[13] M. A. Isa and I. Lazoglu. Five-axis additive manufacturing of freeform models through buildup of transition layers. *Journal of Manufacturing Systems*, 50:69–80, 2019.

[14] Y. Jin, J. Du, Y. He, and G. Fu. Modeling and process planning for curved layer fused deposition. *The International Journal of Advanced Manufacturing Technology*, 91:273–285, 2017.

[15] J. C. Riddick, M. A. Haile, R. Von Wahlde, D. P. Cole, O. Bamiduro, and T. E. Johnson. Fractographic analysis of tensile failure of acrylonitrile-butadiene-styrene fabricated by fused deposition modeling. *Additive Manufacturing*, 11:49–59, 2016.

[16] F. Wasserfall, N. Hendrich, D. Ahlers, and J. Zhang. Topology-aware routing of 3d-printed circuits. *Additive Manufacturing*, 36:101523, 2020.

[17] F. Wulle, D. Coupek, F. Schäffner, A. Verl, F. Oberhofer, and T. Maier. Workpiece and machine design in additive manufacturing for multi-axis fused deposition modeling. *Procedia Cirp*, 60:229–234, 2017.

[18] D. Yadav, D. Chhabra, R. K. Garg, A. Ahlawat, and A. Phogat. Optimization of fdm 3d printing process parameters for multi-material using artificial neural network. *Materials Today: Proceedings*, 21:1583–1591, 2020.

[19] J. Yin, C. Lu, J. Fu, Y. Huang, and Y. Zheng. Interfacial bonding during multi-material fused deposition modeling (fdm) process due to inter-molecular diffusion. *Materials & Design*, 150:104–112, 2018.

[20] X. Zhang and J. Wang. Controllable interfacial adhesion behaviors of polymer-on-polymer surfaces during fused deposition modeling 3d printing process. *Chemical Physics Letters*, 739:136959, 2020.